

Optimization of the EMI shielding effectiveness of fine and ultrafine POFA powder mix with OPC powder using Flower Pollination Algorithm

O L C Narong¹, C K Sia¹, S K Yee³, P Ong², A Zainudin¹, N H M Nor¹ and N A Kasim³

¹ Department of Engineering Design and Materials, University of Tun Hussein Onn Malaysia, Parit Raja 86400, Batu Pahat, Johor, Malaysia

² Department of Mechanic Engineering, University of Tun Hussein Onn Malaysia, Parit Raja 86400, Batu Pahat, Johor, Malaysia

³ Research Centre for Applied Electromagnetic, Faculty of Electrical and Electronic Engineering, University Tun Hussein Onn Malaysia, Parit Raja 86400, Batu Pahat, Johor, Malaysia

E-mail: gd150077@siswa.uthm.edu.my

Abstract. In order to solve the electromagnetic interference (EMI) issue and provide a new application for palm oil fuel ash (POFA), POFA was used as the cement filler for enhancing the EMI absorption of cement-based composites. POFA was refined by using water precipitation for 24 hours to remove the filthiness and distinguish the layer 1 (floated) and layer 2 (sink) of POFA. Both layers POFA were dried for 24 hours at 100 ± 5 °C and grind separately for sieve at 140 μm (Fine) and 45 μm sizes (Ultrafine). The microstructure and element content of the both layers POFA were characterized by scanning electron microscope (SEM) and energy-dispersive X-ray spectroscopy (EDS) respectively. The results showed layer 1 POFA has potentialities for EMI shielding effectiveness (SE) due to its higher carbon content and porous structure. The study reveals that EMI SE also influenced by the particle size of POFA, where smaller particle size can increase 5 % to 13 % of EMI SE. When the specimen consists of 50% POFA with passing through 45 μm sieve, the EMI was shield -13.08 dB in between 50 MHz to 2 GHz range. Flower Pollination Algorithm (FPA) proves that POFA passing 45 μm sieve with 50% mixed to OPC is optimal parameter. The error between experimental and FPA simulation data is below 1.2 for both layers POFA.

1. Introduction

Most of the advance technologies in electrical and electronic devices, especially the wireless and communication systems are polluted by electromagnetic wave (EW) pollution, which can be harmful to health and may cause of death [1], [2]. Electromagnetic interference (EMI) is the disruption of operation of an electronic device when it is in the vicinity of an electromagnetic field (EMF) in the radio frequency (RF) spectrum that is caused by another electronic device. Electromagnetic pollution has become part of people daily life due to the proliferation of the high speed electrical and electronic systems such as a mobile phone based station, mobile phone, radar, television and radio transmitters



and so on that ease our daily life. The studies on electromagnetic fields (EMF) have been motivated primarily by public for health considerations [3]. A high frequency range of electromagnetic wave able to increase human body temperature approximately 1–5 °C. Researchers have reported the severity of the physiological effects produced by the small temperature surge. Some of the effects include, organ malformations, temporary infertility in males, brain lesions, and blood effect [4], [5]. The human brain is sensitive to EMI field and it promotes the brain tumor risk [1], [6]–[8]. Besides that, the device such as cordless telephones, home entertainment systems, computers, and certain medical devices can fail to operate properly in the presence of strong RF fields [8], [9]. Hence, it is important to reduce the EMI radiation.

The current study stated that EMI shielding in building have been shielded by carbon filling cement materials and metal filling cement composite [10]. The carbon filling materials consist of graphite, carbon black, coke and carbon fiber. These carbon materials have comparatively high conductivity and EMI shielding [11]. The metal based fillers consist of metal powder, metal fiber and metal alloys, which are used in cement matrix composites [10]. The metals such as silver, copper, and nickel was used for long time as conductive components in polymer due to their high conductivity [10].

In recent years, Palm oil fuel ash (POFA) is attractive alternative filler commonly found as agricultural waste that is uncontrollably dumped in landfills, especially in South East Asia [12]. As the second largest global palm oil producer, Malaysia has the highest daily wastage [12]. The issue of environmental pollution resulting from disposal of palm oil fuel ash (POFA) has attracted the attention of researchers to explore its potential as an alternative fuel [13] or other field. Some researcher also used the POFA as cement additive or cement replacement as the POFA have similar characteristic with Ordinary Portland Cement (OPC) [12], [14]–[26]. Some researchers have reported that the elements in POFA contribute the most to the microwave absorption is carbon (C) and iron III oxide (Fe_2O_3) [3], [10], [27]–[32].

There are also many other high conductive fillers like silver, copper, and nickel can be use. However, these metal fillers are not only high in cost but very complicated in processing so they are not commonly used in cement matrix composite [10], therefore the POFA was choose to use as filler to mitigate against the EMI. The motivation of using POFA in EMI shielding is to reduce the agricultural waste that is uncontrollably dumped in landfills. Besides that, POFA is containing high carbon and iron III oxide which can be used to prevent the EMF radiation.

The objective of this study is to measure the EMI SE of layer 1 and layer 2 POFA by mixed with OPC at 5%, 20%, 35%, and 50% mixing percentage. Furthermore, this study also to compare the POFA with passing through 140 μm sieve and 45 μm sieve in EMI SE performance after mixed OPC for both layers. The frequency range of the EMI SE measurement is 50 MHz to 2 GHz. At the end of the experiment, the data are optimized by Flower Pollination Algorithm (FPA) method to get the optimum mixing percentage. Lastly, the experimental data were compared to the simulation data for calculating the error.

2. Experimental

2.1 Materials

The main raw material that used in this research is Palm Oil Fuel Ash (POFA) collected from Genting Plantations Oil Mill Ayer Hitam branch in Johor, Malaysia. The palm fibre, palm shell, empty palm fruit bunches burn as fuel at $800\text{ }^\circ\text{C} \pm 50\text{ }^\circ\text{C}$ in the boiler at the palm mill. Ordinary Portland Cement (OPC) type I powder is collected from Civil Engineering Advance Material Laboratory, Faculty of Civil and Environmental Engineering (FKAAS), UTHM. The OPC was used for all sample mixtures.

2.2 POFA Refining Process

One kilogram of POFA is filled into a graduated cylinder. The water from the laboratory is then added into the same cylinder until 80% full. The mixture of POFA and water is stirred for 30 minutes by

using a portable stirrer. After the stirring process, the first-water has been used was removed due to the filthiness in the POFA. Again, the water from the laboratory is then added into the same cylinder until 80% full and left the cylinder for 24-hours. After 24-hour of precipitation, two main layers of POFA appeared, namely layer 1 and layer 2. The layer 1 POFA was withdrawn using a spatula as it is floated. Then layers 2 was removed by using a syringe withdrawal method as given in Figure 1 [33].

After separating the layers of POFA, POFA was placed in different containers. Then, the POFA layer 1 and layer 2 was drying in oven for 24 hours at temperature of 100°C. Due to the high humidity of POFA, the drying time must be 24 hours and above. This is to make sure the POFA is completely dry and to avoid the stickiness during grinding process.

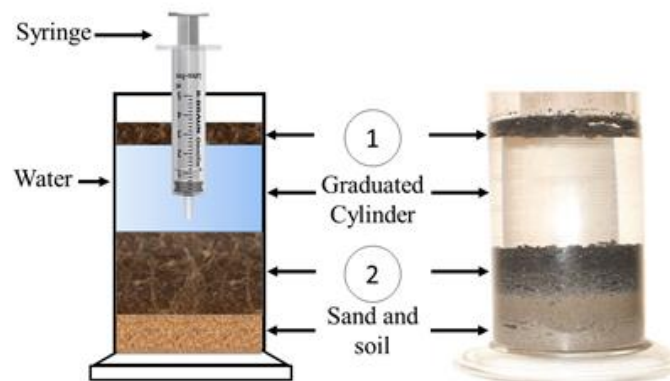


Figure 1: Schematic diagram of syringe withdrawal method, (1) Layer 1 and (2) Layer 2

2.3 Physical properties and chemical compositions of POFA

All layers were examined by Energy Dispersive X-ray Spectroscopy (EDS) to identify the element's content of three random point in the POFA. Then the microstructure characteristic of each layer was explored using Scanning Electron Microscope (SEM).

2.4 Sample preparation

After drying process, both layers were grind using planetary micro mill Pulverisette 7 Classic Line machine. The grinding speed is 250 RPM with 10 grinding balls. After grinding process, the POFA was sieved by using Vibratory Sieve Shake Analysette 3 Pro. The sieve sizes are 140 μm and 45 μm . Both layers were sieved separately with the selected sieve size. The POFA passing through 140 μm sieve was declared as Fine POFA (FP) and POFA passing through 45 μm sieve was declared as Ultrafine POFA (UP). After sieving process, the OPC is partially replaced by POFA at the ratio of 5%, 20%, 35% and 50%. The detail of all samples is given in Table 1 to Table 4. Detail in Table 1 and Table 2 are for POFA layer 1 and detail in Table 3 and Table 4 for POFA layer 2. The 100% OPC was represented as CP where the CP is used as reference for other samples. CPF is representing OPC mixed with Fine POFA and CPU is representing OPC mixed with Ultrafine POFA.

Table 1: The mixing ratio of CPF and OPC for layer 1

Name of the samples	% Weight of cement (OPC)	% Weight of layer 1 POFA based on particle size (FP)
CP 100%	100	0
1-CPF 5%	95	5
1-CPF 20%	80	20
1-CPF 35%	65	35
1-CPF 50%	50	50

Table 2: The mixing ratio of CPU and OPC for layer 1

Name of the samples	% Weight of cement (OPC)	% Weight of layer 1 POFA based on particle size (UP)
CP 100%	100	0
1-CPU 5%	95	5
1-CPU 20%	80	20
1-CPU 35%	65	35
1-CPU 50%	50	50

Table 3: The mixing ratio of CPF and OPC for layer 2

Name of the samples	% Weight of cement (OPC)	% Weight of layer 2 POFA based on particle size (FP)
CP 100%	100	0
2-CPF 5%	95	5
2-CPF 20%	80	20
2-CPF 35%	65	35
2-CPF 50%	50	50

Table 4: The mixing ratio of CPU and OPC for layer 2

Name of the samples	% Weight of cement (OPC)	% Weight of layer 1 POFA based on particle size (UP)
CP 100%	100	0
2-CPU 5%	95	5
2-CPU 20%	80	20
2-CPU 35%	65	35
2-CPU 50%	50	50

2.5 Transmission Measurement

Transmission measurement (S_{21}) is the experimental measurement method of the SE. SE can separate into the product of three terms each represents one of the phenomena of reflection loss (R_{dB}), absorption loss (A_{dB}) and multiple reflection loss (M_{dB}) [10]. The SE of a shield is defined in decibels (dB) and its magnitude can be writes as $SE_{dB} = R_{dB} + A_{dB} + M_{dB}$ [10]. The signal is in the radio frequency (RF) form. The RF was supplied from port 1 to port 2 where the sample is placed in between the port 1 and port 2 transmission lines. Hundreds of data were obtained by Network Analyser (NA) and calculated in MATLAB by using equation (1). APC-7 connectors are used due to the samples are in powder form. This measurement carried out by using APC 7 connectors as sample holder. During this measurement, both APC 7 connectors are connected to a NA. NA is a device used to measure the ratio of transmission and reflection of electromagnetic waves through a device under test. In this work the device under test is the APC 7 connectors. The APC 7 connectors are shown in Figure 2. Figure 3 shows how the powder-formed-samples are placed in the APC 7 connector.



Figure 2: APC 7 connector tail (1) and head (2)

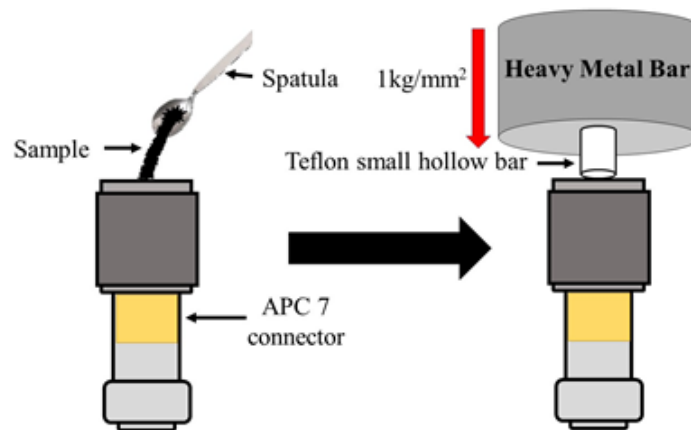


Figure 3: The method of insert sample into the APC 7 connector

The inner diameter of the APC 7 connector 3 mm and outer diameter is 7 mm. The sample is toroidal form when it is inside the APC 7 connector. The sample in the APC 7 connectors is compressed by using a heavy metal bar, where the pressing load approximately 1 kg/mm^2 . This is to ensure the sample is completely occupied in the APC-7 connector space. After the measurement is completed, the APC-7 connector was clean by using high pressure air. The blow process was needed to remove the remaining sample in the APC 7 connector before the next measurement. Figure 4 shown the schematic diagram of dielectric measurement method. In this measurement the SE is obtained based on equation (1). S_{21} represents the power reserved at antenna 2 relative to the power input to antenna 1. Two types of S_{21} here, which are $S_{21\text{-without}}$ and $S_{21\text{-with}}$. $S_{21\text{-without}}$ representing the S_{21} when the APC 7 connector does not contain any sample, while $S_{21\text{-with}}$ represent the S_{21} when the APC 7 connector is filled with the sample which is in the powder form.

$$SE(\text{dB}) = \text{Forward gain} = 20 \log \left[\frac{S_{21\text{-with}}}{S_{21\text{-without}}} \right] \quad (1)$$

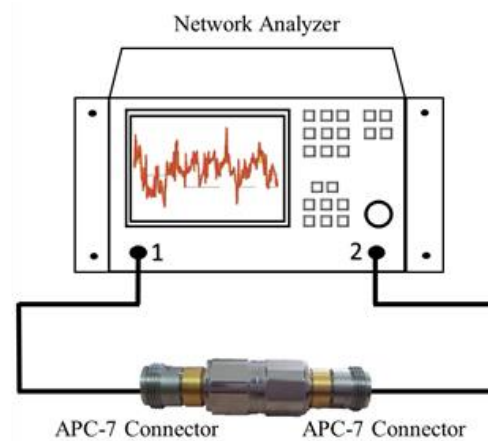


Figure 4: Schematic diagram of transmission measurement method

2.6 Flower pollination algorithm (FPA)

FPA was developed by Xin-She Yang in 2012 [34]. This algorithm method is a new nature-inspired algorithm, based on the characteristics of flowering plants [34], [35]. Flower pollination algorithm (FPA) uses the following four rules in optimization [34]:

- Biotic and cross-pollination can be considered as a process of global pollination process, and pollen-carrying pollinators move in a way which obeys Lévy flights (Rule 1).
- For local pollination, abiotic and self-pollination are used (Rule 2).
- Pollinators such as insects can develop flower constancy, which is equivalent to a reproduction probability that is proportional to the similarity of two flowers involved (Rule 3).
- The interaction or switching of local pollination and global pollination can be controlled by a switch probability $p \in [0, 1]$, with a slight bias towards local pollination (Rule 4).

To run the FPA, a set of objective function equation must develop before running the optimization in MATLAB software. The objective function equation is as equation (2) shown. This objective function equation was developed in Microsoft Excel.

$$Y = b_0 + b_1x_1 + b_2x_2 + b_3x_1x_2 \quad (2)$$

where Y is the dependent variable or estimation for the response variables of the designed experiment (EMI shielding effectiveness), and b is the estimation for the regression coefficient computed by least squares approach. The pseudo code of the proposed Flower Pollination Algorithm (FPA) can represent as follows [34]:

```

Objective min or max  $f(\mathbf{x})$ ,  $\mathbf{x} = (x_1, x_2, \dots, x_d)$ 
Initialize a population of  $n$  flowers/pollen gametes with random solutions
Find the best solution  $g^*$  in the initial population
Define a switch probability  $p \in [0, 1]$ 
Define a stopping criterion (either a fixed number of generations/iterations or accuracy)
while ( $t < \text{MaxGeneration}$ )
    for  $i = 1: n$  (all  $n$  flowers in the population)
        if  $\text{rand} < p$ ,
            Draw a ( $d$ -dimensional) step vector  $L$  which obeys a Lévy distribution

```

```

    Global pollination via  $x_i^{t+1} = x_i^t + L(g_* - x_i^t)$ 
else
    Draw  $\epsilon$  from a uniform distribution in  $[0,1]$ 
    Do local pollination via  $x_i^{t+1} = x_i^t + \epsilon(x_j^t - x_k^t)$ 
end if
Evaluate new solutions
If new solutions are better, update them in the population
end for
Find the current best solution  $g_*$ 
end while
Output the best solution found

```

3 Results and discussions

3.1 Physical properties and chemical compositions of POFA

The EDS and SEM result were discussed in this subsection. From the precipitation process, the POFA is split into two main layers as in Figure 5. Based on the EDS result (Table 5), the carbon content of layer 1 is higher than layer 2, which is 85.89%. Figure 6 shows the SEM morphology images of both layers. It can be seen that the layer 1 (Figure 6 (1)) shows that the particle is fully porous like light foam. This explains the reason why layer 1 is floating on the surface. The SEM morphology image of layer 2 (Figure 6 (2)) shows less porous compared to layer 1. It is observed that layer 2 still contains the unburn palm shell and this is the reason layer 2 was submerged in the water.



Figure 5: The layer of POFA, (1) Layer 1 and (2) Layer 2

Table 5: Compound in each layer of POFA

Compound	Layer 1 (%)	Layer 2 (%)
C	85.89	81.68
MgO	1.27	1.12
Al ₂ O ₃	-	1.72
SiO ₂	5.60	8.22
P ₂ O ₅	-	-
K ₂ O	3.25	2.52
CaO	3.98	2.01
FeO	-	2.73
Total	100	100

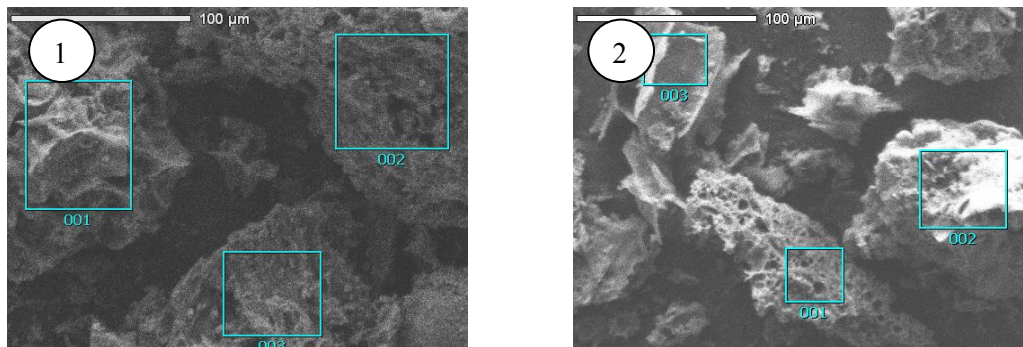


Figure 6: SEM morphology image of (1) layer 1 and (2) layer 2 POFA

3.2 Experimental SE measurement

The SE of POFA mix with OPC for layer 1 (CPU vs CPF) was shown in Figure 7. The results show that all ultrafine POFA samples (CPU) were achieved better SE than fine POFA (CPF). For POFA layer 1, the ultrafine POFA (CPU) can increase the SE approximately at 13%. The results show that the different particle size of POFA can improve the SE. The highest SE was achieved by ultrafine POFA (CPU) at 50% of mixing ratio, about -13.53 dB SE at 1.52 GHz. The fine POFA (CPF) layer 1 mix OPC with 50% of the ratio can achieve only -12.11 dB at 2 GHz.

The SE of POFA mix with OPC for layer 2 (CPU vs CPF) was shown in Figure 8. The results also show that all ultrafine POFA samples (CPU) were achieved better SE than fine POFA (CPF). This result was the same pattern as layer 1 because ultrafine POFA (CPU) has better SE than fine POFA (CPF). The ultrafine POFA (CPU) can increase the SE approximately at 5 %. The highest SE for layer 2 was achieved by ultrafine POFA (CPU) at 50% of mixing ratio, about -12.82 dB SE at 2 GHz. The fine POFA (CPF) layer 1 mix OPC with 50% of the ratio can achieve -12.46 dB at 1.5 GHz.

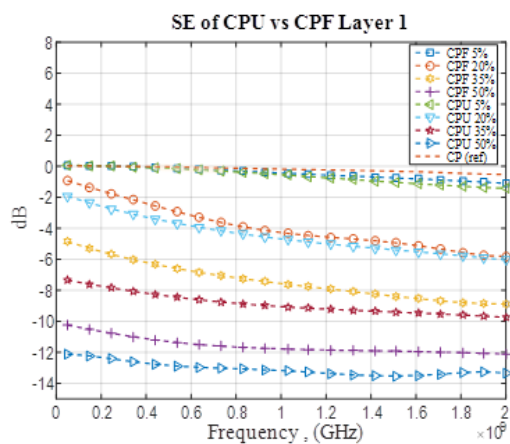


Figure 7: Shielding effectiveness of layer 1 (CPU vs CPF)

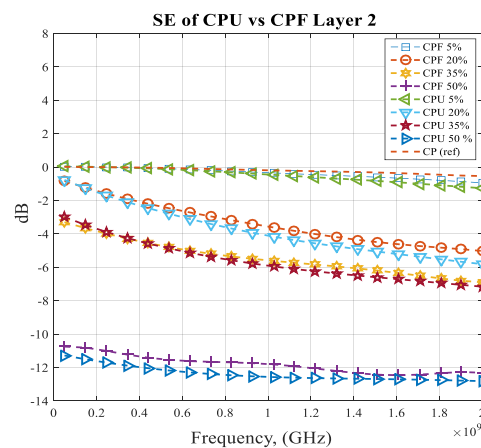


Figure 8: Shielding effectiveness of layer 2 (CPU vs CPF)

In Figure 9 and Figure 10, POFA layer 1 shows better SE results because of the layer 1 POFA has the high carbon content. With the existence of carbon in POFA, this helps to transform the EM field into heat [21], [27], as the carbon has good conductivity [36], [37]. The carbon was found in both layers of POFA. The carbon/carbon black has been used as floor heating elements, electronic equipment related material in various display components and magnetic recording materials [36], and electromagnetic interference (EMI) shielding [37]. Overall results were proving that the POFA replacement in OPC can improve the SE compared to the 100% OPC (CP). The smaller particle size

POFA can improve with a certain percentage of SE because of the small particle can fulfill the space and giving a good shielding especially in complex space. Overall, the layer 1 POFA show better SE compare layer 2 POFA.

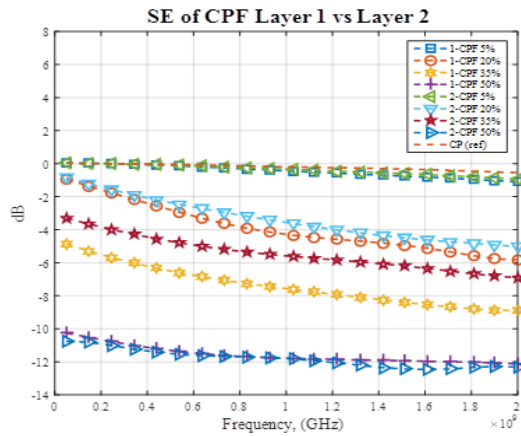


Figure 9: Shielding effectiveness of CPF (Layer 1 vs Layer 2)

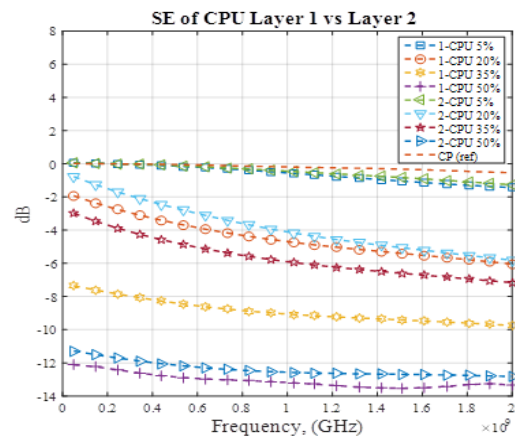


Figure 10: Shielding effectiveness of CPU (Layer 1 vs Layer 2)

3.3 FPA optimization and simulation

In this subsection was discussing about the FPA optimization results. This optimization method was used to validate the experimental and FPA simulation data. In addition, the FPA can obtain the optimal sieve size and optimal mixing ratio POFA in OPC for EMI SE. Table 6 shows the regression statistics result for POFA layer 1, where the R square is equal to 0.998733, which is a perfect fit. The biggest SE value (with ignore the positive and negative sign), the better regression line fit the data. From the analysis of variance (ANOVA) at Table 7 shown, the result is statistically significant due to the significant F value less than 0.05. In addition, all variables are significant to the EMI SE due to three over four P value less than 0.05. Base on the Table 8, the sign and magnitude of regression coefficient signify the relative influence of each parameter of the output response (EMI SE) with a negative sign indicating an antagonistic effect whilst a positive one signifies a synergistic effect. The mathematical interaction model of EMI SE of POFA layer 1 was developed based on the sign and magnitude of regression coefficient as shown in equation (3).

$$Y = b_0 + b_1x_1 + b_2x_2 + b_3x_1x_2$$

$$Y = -6.311 + 0.458x_1 + -5.901x_2 + 0.371x_1x_2 \quad (3)$$

Table 6: Regression Statistics for layer 1

Regression Statistics	
Multiple R	0.999367
R Square	0.998733
Adjusted R Square	0.997784
Standard Error	0.223131
Observations	8

Table 7: ANOVA for layer 1

	df	SS	MS	F	Significance F
Regression	3	157.0416	52.34719	1051.418	3.01E-06
Residual	4	0.199149	0.049787		
Total	7	157.2407			

Table 8: Objective function information for layer 1

Variable	Coefficients	Standard Error	t Stat	P-value	Lower 95%	Upper 95%	Lower 95.0%	Upper 95.0%
b0	-6.311	0.079	-79.993	0.000	-6.530	-6.092	-6.530	-6.092
b1	0.458	0.079	5.806	0.004	0.239	0.677	0.239	0.677
b2	-5.901	0.106	-55.752	0.000	-6.195	-5.607	-6.195	-5.607
b3	0.371	0.106	3.507	0.025	0.077	0.665	0.077	0.665

For layer 1, the prediction result suggested that 45 μm sieve size and 50% of mixing ratio is the optimum value in SE for layer 1. This is the same with experimental result where experimental result also shows better SE at 45 μm sieve size and 50% of mixing ratio. The SE from FPA optimization method is -13.04 dB where it has just obtained only 0.04 error compare to the experimental result. The target has set to achieve -14 dB, but the optimization result only obtains -13.04 dB.

Table 9 shows the regression statistics result for POFA layer 2, where the R square is equal to 0.937431098, which is a practicable fit. From the analysis of variance (ANOVA) at Table 10 shown, the POFA layer 2 also statistically significant due to the significant F value less than 0.05. In addition, all variables are considered significant to the EMI SE due to the two over four P value less than 0.05 but well less than POFA layer 1. Base on the Table 11, the sign and magnitude of regression coefficient signify the relative influence of each parameter of the output response (EMI SE) with a negative sign indicating an antagonistic effect whilst a positive one signifies a synergistic effect which is the same trend with POFA layer 1. The mathematical interaction model of EMI SE for POFA layer 2 was developed as shown in equation (4).

$$Y = b_0 + b_1x_1 + b_2x_2 + b_3x_1x_2$$

$$Y = -5.436 + 0.171x_1 + -5.542x_2 + 0.080x_1x_2 \quad (4)$$

Table 9: Regression Statistics for layer 2

Regression Statistics	
Multiple R	0.968210255
R Square	0.937431098
Adjusted R Square	0.890504422
Standard Error	1.510563977
Observations	8

Table 10: ANOVA for layer 2

	df	SS	MS	F	Significance F
Regression	3	136.7473959	45.58247	19.97651	0.007185
Residual	4	9.127214114	2.281804		
Total	7	145.87461			

Table 11: Objective function information for layer 2

Variable	Coefficients	Standard Error	t Stat	P-value	Lower 95%	Upper 95%	Lower 95.0%	Upper 95.0%
b0	-5.436	0.534	-10.178	0.001	-6.918	-3.953	-6.918	-3.953
b1	0.171	0.534	0.320	0.765	-1.312	1.654	-1.312	1.654
b2	-5.542	0.717	-7.734	0.002	-7.531	-3.552	-7.531	-3.552
b3	0.080	0.717	0.111	0.917	-1.910	2.069	-1.910	2.069

For POFA layer 2, the prediction result also suggested that 45 μm sieve size and 50% of mixing ratio is the optimum value in SE. The SE from FPA optimization method is -11.23 dB where the 1.16 error is compared to the experimental result. In the FPA software, the target has set to achieve -14 dB, but the optimization result only obtains -11.23 dB. Table 12 shows the comparison of SE between FPA simulation and experimental data.

Table 12: Comparison of SE between FPA simulation and experimental data

Samples name	Layers	Sieve sizes (μm)	Mixing percentages (%)	EMI SE Average (dB)		Error
				FPA Simulation	Experimental	
1-CPU 50%	1	45	50%	-13.04	-13.08	0.04
2-CPU 50%	2	45	50%	-11.23	-12.39	1.16

4. Conclusion

In conclusion, this study has proven that the POFA has the potential to be used as the additive for cement based material to enhance the EMI SE in the building. The element that contributed the most to EMI SE in POFA is carbon as the carbon has good conductivity. The high porosity of particle in POFA also gives a good absorbing to the EMF. The highest SE was achieved by layer 1 ultrafine POFA (CPU) with passing 45 μm sieve at 50% of mixing ratio, about -13.53 dB at 1.52 GHz. While the fine POFA (CPF) layer 1 mix OPC with 50% of the ratio can achieve only -12.11 dB at 2 GHz. The layer 1 POFA shows better EMI SE compare to layer 2 POFA because the layer 1 POFA contain higher carbon content. This study has found that the smaller particle size of POFA can improve the SE in 5% to 13% due to the smaller particle. The smaller particle POFA can cover up the complex space in the cement structure to avoid the EMF leaked. Based on FPA simulation data, the error is below 1.2 for both layers. FPA optimization prediction has come out comparable result with experimental data. By using FPA optimization method can help researcher obtain the optimum sieve size and mixing percentage. This is a good sign to improve the next study.

Acknowledgment

This research was financed by Fundamental Research Grant Scheme (FRGS) Vot No. 1490 and Office for Research, Innovation, Commercialization and Consultancy Management (ORICC).

References

- [1] C. Beall, E. Delzell, P. Cole, and I. Brill, "Brain tumors among electronics industry workers.," *Epidemiology*, vol. 7, no. 2, pp. 125–130, 1996.
- [2] S. Xie, Y. Yang, G. Hou, J. Wang, and Z. Ji, "Development of layer structured wave absorbing mineral wool boards for indoor electromagnetic radiation protection," *J. Build. Eng.*, vol. 5, pp. 79–85, 2016.
- [3] G. Bantsis, C. Sikalidis, M. Betsiou, T. Yioultsis, and T. Xenos, "Electromagnetic absorption,

- reflection and interference shielding in X-band frequency range of low cost ceramic building bricks and sandwich type ceramic tiles using mill scale waste as an admixture,” *Ceram. Int.*, vol. 37, no. 8, pp. 3535–3545, 2011.
- [4] T. Wessapan, S. Srisawatdhisukul, and P. Rattanadecho, “Numerical analysis of specific absorption rate and heat transfer in the human body exposed to leakage electromagnetic field at 915 MHz and 2450 MHz,” *J. Heat Transfer*, vol. 133, no. 5, p. 51101, 2011.
- [5] P. Keangin, K. Vafai, and P. Rattanadecho, “Electromagnetic field effects on biological materials,” *Int. J. Heat Mass Transf.*, vol. 65, pp. 389–399, 2013.
- [6] D. P. Loomis and D. A. Savitz, “Mortality from brain cancer and leukaemia among electrical workers,” *Br. J. Ind. Med.*, vol. 47, no. 9, pp. 633–8, 1990.
- [7] B. B. Levitt and H. Lai, “Biological effects from exposure to electromagnetic radiation emitted by cell tower base stations and other antenna arrays,” *Environ. Rev.*, vol. 18, no. NA, pp. 369–395, 2010.
- [8] E. E. Fesenko, V. R. Makar, E. G. Novoselova, and V. B. Sadovnikov, “Microwaves and cellular immunity. I. Effect of whole body microwave irradiation on tumor necrosis factor production in mouse cells,” *Bioelectrochem. Bioenerg.*, vol. 49, no. 1, pp. 29–35, 1999.
- [9] A. Miszczyk and K. Darowicki, “Study of anticorrosion and microwave absorption properties of NiZn ferrite pigments,” *Anti-Corrosion Methods Mater.*, vol. 58, no. 1, pp. 13–21, 2011.
- [10] H. Guan, S. Liu, Y. Duan, and J. Cheng, “Cement based electromagnetic shielding and absorbing building materials,” *Cem. Concr. Compos.*, vol. 28, no. 5, pp. 468–474, 2006.
- [11] D. D. L. Chung, “Materials for electromagnetic interference shielding,” *J. Mater. Eng. Perform.*, vol. 9, no. 3, pp. 350–354, 2000.
- [12] N. H. A. Khalid, M. W. Hussin, J. Mirza, N. F. Ariffin, M. A. Ismail, H.-S. Lee, A. Mohamed, and R. P. Jaya, “Palm oil fuel ash as potential green micro-filler in polymer concrete,” *Constr. Build. Mater.*, vol. 102, pp. 950–960, 2016.
- [13] W. A. N. W. Mohamed and N. R. Abdullah, “Combustion Characteristics of Palm Shells and Palm Fibers Using an Inclined Grate Combustor,” *Carbon N. Y.*, vol. 57, pp. 48–94.
- [14] A. S. M. A. Awal, I. A. Shehu, and M. Ismail, “Effect of cooling regime on the residual performance of high-volume palm oil fuel ash concrete exposed to high temperatures,” *Constr. Build. Mater.*, vol. 98, pp. 875–883, 2015.
- [15] S. K. Nguong and U. Teknologi, “A Short-Term Investigation On High Volume Palm Oil Fuel Ash (POFA) Concrete,” *35th Conf. OUR WORLD Concr. Struct. 25 - 27 August 2010, Singapore*, 2010.
- [16] W. Tanchirapat, T. Saeting, C. Jaturapitakkul, K. Kiattikomol, and A. Siripanichgorn, “Use of waste ash from palm oil industry in concrete,” *Waste Manag.*, vol. 27, no. 1, pp. 81–88, 2007.
- [17] V. Sata, C. Jaturapitakkul, and K. Kiattikomol, “Utilization of palm oil fuel ash in high-strength concrete,” *J. Mater. Civ. Eng.*, vol. 16, no. 6, pp. 623–628, 2004.
- [18] M. A. Salih, A. A. Abang Ali, and N. Farzadnia, “Characterization of mechanical and microstructural properties of palm oil fuel ash geopolymer cement paste,” *Constr. Build. Mater.*, vol. 65, pp. 592–603, 2014.
- [19] N. Ranjbar, A. Behnia, B. Alsubari, P. Moradi Birgani, and M. Z. Jumaat, “Durability and mechanical properties of self-compacting concrete incorporating palm oil fuel ash,” *J. Clean. Prod.*, vol. 112, pp. 723–730, 2015.
- [20] M. A. A. Rajak, Z. A. Majid, and M. Ismail, “Morphological Characteristics of Hardened Cement Pastes Incorporating Nano-palm Oil Fuel Ash,” *Procedia Manuf.*, vol. 2, no. February, pp. 512–518, 2015.
- [21] H. Noorvand, A. A. A. Ali, R. Demirboga, H. Noorvand, and N. Farzadnia, “Physical and chemical characteristics of unground palm oil fuel ash cement mortars with nanosilica,” *Constr. Build. Mater.*, vol. 48, pp. 1104–1113, 2013.
- [22] A. Awal and S. K. Nguong, “A short-term investigation on high volume palm oil fuel ash (POFA) concrete,” *Proc. 35th Conf. our World Concr. Struct.*, pp. 185–192, 2010.

- [23] K. Muthusamy and Z. N. Azzimah, "Exploratory Study of Palm Oil Fuel Ash as Partial Cement Replacement in Oil Palm Shell Lightweight Aggregate Concrete," vol. 8, no. 2, pp. 150–152, 2014.
- [24] M. R. Karim, M. F. M. Zain, M. Jamil, and F. C. Lai, "Fabrication of a non-cement binder using slag, palm oil fuel ash and rice husk ash with sodium hydroxide," *Constr. Build. Mater.*, vol. 49, pp. 894–902, 2013.
- [25] P. Chindaprasirt, S. Rukzon, and V. Sirivivatnanon, "Resistance to chloride penetration of blended Portland cement mortar containing palm oil fuel ash, rice husk ash and fly ash," *Constr. Build. Mater.*, vol. 22, no. 5, pp. 932–938, 2008.
- [26] S. Bamaga, M. A. Ismail, and M. W. Hussin, "Chloride Resistance of Concrete Containing Palm Oil Fuel Ash," vol. 1, no. December, pp. 158–166, 2010.
- [27] H. Abdullah, A. Zanal, M. N. Taib, I. R. Mohamed Noordin, W. K. Wan Ali, R. Ariffin, S. Abdullah, R. Baharudin, and A. T. Abdullah, "Microwave Absorber Coating Material Using Oil Palm Ash," *Adv. Mater. Res.*, vol. 512–515, pp. 1941–1944, 2012.
- [28] L. Baoyi, D. Yuping, and L. Shunhua, "The electromagnetic characteristics of fly ash and absorbing properties of cement-based composites using fly ash as cement replacement," *Constr. Build. Mater.*, vol. 27, no. 1, pp. 184–188, 2012.
- [29] R. Che, C. Wang, Y. Ni, and B. Yu, "Preparation and microwave absorbing properties of the core-nanoshell composite absorbers with the magnetic fly-ash hollow cenosphere as core," *J. Environ. Sci.*, vol. 23, pp. S74–S77, 2011.
- [30] Z. Dou, G. Wu, X. Huang, D. Sun, and L. Jiang, "Electromagnetic shielding effectiveness of aluminum alloy–fly ash composites," *Compos. Part A Appl. Sci. Manuf.*, vol. 38, no. 1, pp. 186–191, 2007.
- [31] M. Mishra, A. P. Singh, and S. K. Dhawan, "Expanded graphite–nanoferrite–fly ash composites for shielding of electromagnetic pollution," *J. Alloys Compd.*, vol. 557, pp. 244–251, 2013.
- [32] J. Y. Cao and D. D. L. Chung, "Use of fly ash as an admixture for electromagnetic interference shielding," *Cem. Concr. Res.*, vol. 34, no. February, pp. 1889–1892, 2004.
- [33] M. B. Melwanki and M. R. Fuh, "Dispersive liquid-liquid microextraction combined with semi-automated in-syringe back extraction as a new approach for the sample preparation of ionizable organic compounds prior to liquid chromatography," *J. Chromatogr. A*, vol. 1198–1199, no. 1–2, pp. 1–6, 2008.
- [34] X. S. Yang, M. Karamanoglu, and X. He, "Multi-objective flower algorithm for optimization," *Procedia Comput. Sci.*, vol. 18, pp. 861–868, 2013.
- [35] X.-S. Yang, "Flower pollination algorithm for global optimization," in *International Conference on Unconventional Computing and Natural Computation*, 2012, pp. 240–249.
- [36] W. Zhang, A. A. Dehghani-Sanij, and R. S. Blackburn, "Carbon based conductive polymer composites," *J. Mater. Sci.*, vol. 42, no. 10, pp. 3408–3418, 2007.
- [37] S. K. De and J. R. White, *Short fibre-polymer composites*. Elsevier, 1996.